

Sulfation-Roasting-Leaching of Brazilian Nickel Laterite Ore

Pedro Paulo Medeiros Ribeiro¹, Souza L. C. M.¹, Santos I. D.², Radino-Rouse², and Dutra A. J. B.¹

1. Federal University of Rio de Janeiro, Brazil

2. Instituto Tecnológico Vale/Vale S.A, Brazil

Abstract: Exploitation of nickel from laterite ore resources has increased due to the depletion of high grade nickel sulfide ores. A hydro-pyrometallurgical route was applied in a sample of Brazilian laterite ore. The sample was pugged with sulfuric acid, subjected to a pre-roasting around 265°C, roasting around 690°C followed by water leaching. The operational parameters investigated were: leaching pH, acid amount; salt additions, particle size. Under favorable conditions nickel recoveries around 86% were achieved. These recoveries are strongly dependent on the particle size and sulfuric acid concentration due to the high amount of magnesia in the ore.

Key words: laterite ore, hydro-pyrometallurgical route, nickel

1. Introduction

Nickel can be obtained from sulfide or laterite ores. Sulfides reserves are the primary nickel resources, however, due to the decrease in nickel grade and the number of reserves, laterite ores have attracted attention [1].

Laterites are consisted by oxide, hydroxide and silicates minerals. Its main deposits are located in equatorial regions and were formed by the weathering of rocks such as olivene [1]. Nickel in laterite ore appears associated with many minerals as chlorite and goethite and there is no nickel mineral in laterite ores [2]. Table 1 shows the main minerals found in laterite ores.

Laterite composition changes according to the deep of the layer and the weather of the region. The laterite ore can be divided into three different types: limonitic, transition and saprolitic [4].

- Limonitic layer: this layer is constituted mainly of oxides, and hydroxides, principally goethite which can be represented by the following formula, FeOOH . Nickel and cobalt concentration in this layer is small and the iron concentration is high.
- Transition layer: It is a transition layer between the limonitic and the saprolitic one. This layer is dominated by smectites and nickel, cobalt, and magnesium content increases while iron content decreases [5].
- Saprolitic layer: It is the deeper layer found in laterite ores. It is dominated by silicates minerals and it is rich in magnesium. Nickel and cobalt content in this layer is also higher than in the other ones of laterite ores and it is characterized by heterogeneous composition.

The average chemical composition of some laterite ores can be seen in Table 2. It is possible to observe that the limonitic ores exhibit iron content equal to or higher than 29% while nickel content is found in the range from 0.12 to 1.5%. For the saprolitic laterite ores,

Corresponding author: Pedro Paulo Medeiros Ribeiro, Master of Science; research areas/interests: extractive metallurgy. E-mail: rppp.19999@gmail.com.

iron content is smaller while nickel and magnesium contents are higher.

Table 1 Main minerals found in laterite ores [3].

Main minerals	Goethite: $\alpha - \text{FeOOH}$, Hematite: $\alpha - \text{Fe}_2\text{O}_3$ Maghemite: $\gamma - \text{Fe}_3\text{O}_4$ Chromite: FeCr_2O_4 Garnierite: $(\text{Ni}, \text{Mg})\text{SiO}_3 \cdot n\text{H}_2\text{O}$ Serpentine: $(\text{Mg}, \text{Al}, \text{Fe}, \text{Mn}, \text{Ni})_{2-3}(\text{Si}, \text{Al}, \text{Fe})_2\text{O}_5(\text{OH})_4$ Smectite: $\text{Mg}_{0.2}(\text{Fe}_{1.2}\text{Mg}_{0.5}\text{Ni}_{0.1}\text{Al}_{0.3})(\text{Si}_{3.8}\text{Al}_{0.2})\text{O}_{10}(\text{OH})_{2.2}\text{H}_2\text{O}$ Asbolane: $(\text{Co}, \text{Ni})_{1-y}(\text{MnO}_2)_{2-x}(\text{OH})_{2-2y+2x}\text{H}_2\text{O}$ Lithiophorite: $(\text{Al}, \text{Li})\text{MnO}_2(\text{OH})_2$ Ringwoodite: $(\text{Mg}, \text{Fe})_2\text{SiO}_4$ Nontronite: $\text{Na}_{0.3}\text{Fe}_2\text{Si}_4\text{O}_{10}(\text{OH})_2 \cdot 4\text{H}_2\text{O}$ Phlogopite: $\text{KMg}_3(\text{Si}_3\text{Al})\text{O}_{10}(\text{OH})_2$ Caunilite: $\text{Al}_4\text{Si}_4\text{O}_{10}(\text{OH})_8$ Chlorite: $(\text{Mg}, \text{Fe}, \text{Al}, \text{Ni})_{5-6}(\text{Si}, \text{Al})_4\text{O}_{10}(\text{OH})_8$
---------------	--

Table 2 Average chemical composition of laterite ores. (a) ([3]); (b) ([6]); (c) ([7]); (d) ([8]).

Type	Composition (w/w)								
	Ni	Co	Fe	S	SiO ₂	MgO	Al ₂ O ₃	CuO	Cr ₂ O ₃
Limonitica	1-1.5	0.1-0.2	> 40		6	3	6		
Saprolitica	2.4	0.05	< 15		38	25			
Limonitica	1.3	0.083	29	0.43	28.8	2.26	5.83	0.039	1.9
Saprolitica	1.2	0.044	16	< 0.01	44.9	6.91	4.17	0.009	0.99
Limoniticb	1.7	0.15	> 40		6	3			
Limoniticc	0.12	0.14	46				1.6		
Limoniticc	1.2	0.16	48	0.4	3.2	0.6	2.05		1.65
Lateritidd	0.96	0.1	48.5			1.12	3.94		0.71
Lateritidd	1.23	0.09	33.5			6.39	2.89		0.68

There are many routes to extract nickel from laterite ores such as high pressure acid leaching (HPAL), heap leaching, organic leaching, pyrometallurgy routes, and many others. To choose the most suitable route it is necessary to know the mineral and chemical compositions, particle size and, especially, costs.

The aim of this work was to investigate the efficiency of the sulfation-roasting-leaching route for nickel and cobalt extraction of a Brazilian laterite sample focusing on the amount of sulfuric acid used.

2. Material and Methods

2.1 Experimental Procedure

Initially, a sample of a Brazilian laterite nickel ore was quartered and wet deagglomerated and dried in an oven at 75°C during 24 hours. Then, part of the sample was classified by sieving in a Rot-tap for 15 minutes. The target was to separate particles fraction smaller

than 75 μm . The other fraction of the sample was divided in two fractions: one grinded to 100% below — 38 μm and the other just deagglomerated, without sieving. These three sub-samples were subjected to pre-roasting, roasting and leaching. For these steps, the following procedure was adopted: 1 g of the sample was added to a porcelain crucible to which was added a pre-established amount of water (10 or 40% (w/w)), then, sulfuric acid additions ranging from 34 to 68% (w/w) were slowly mixed under continuous agitation. The pug was heated, in a muffle furnace (Carbolite 1200), for the pre-roasting and roasting. The pre-roasting was carried out in a temperature range of 100 to 455°C from 20 to 60 minutes. Then, the samples were cooled to room temperature, deagglomerated and roasted at temperatures ranging from 620°C to 690°C during 20 minutes. The samples from the roasting step were leached with water or acidulated water ($0.8 < \text{pH}$

< 1.5), with a solid to liquid ratio of 1 to 40, in a temperature range of 25°C to 90°C for 30 minutes under continuous magnetic stirring (340 rpm). After leaching, the pulp was filtered and the solid residue was dried and weighted, while the metals content in the pregnant solution were determined by atomic absorption. After filtration, the solutions pH was kept below 2 to avoid nickel precipitation. The magnesium, nickel, iron and cobalt recoveries in the pregnant

solution were determined by equation (1) from the metals content presented in Table 3. The HSC software, version 8.2, was employed for the thermodynamic analysis.

$$\text{Recovery} = \frac{t_{ml}}{t_{mm}} * 100 \quad (1)$$

where, t_{ml} is the metal content in the pregnant solution and t_{mm} the metal content in the ore.

Table 3 Magnesium, nickel, iron and cobalt content of nickel laterite ore sample (w/w).

	Mg (w/w)	Ni (w/w)	Fe (w/w)	Co (w/w)
d < 75µm	5.03	2.09	37.49	0.09
Head	5.08	1.72	29.30	0.09

The mineralogical and chemical characterization of the raw samples as of the products obtained were done by Scanning Electron Microscope (SEM) — coupled to Energy Dispersive X-Ray Spectroscopy (EDS) — MEV (JEOL-JSM 6460), X-ray diffraction analyses were performed with a Shimadzu XRD-6000 with copper radiation in the range from 10° to 90° (2θ) with 0.02 steps and count of 0.6 s per step. Chemical analyses were carried out by atomic absorption spectroscopy— EAA (Shimadzu AA 6800).

The pore size analysis was done using the Image J software and the comminution was done manually using an agate grinding media.

3. Results and Discussion

SEM image of the laterite ore as received showing the particles agglomeration is shown in Fig. 1. It is possible to observe particles with spherical, needle and plate formats representing hematite, goethite, and quartz, respectively as identified by EDS analysis and not showed here.

SEM image of the laterite sample after deagglomeration with water before and after image processing can be seen in Fig. 2. In Fig. 2A it is shown the image as acquired by SEM, in Fig. 2B after the threshold (transformation to grayscale) and Fig. 3C after the application of some filters such high pass and median. The use of filters helps to emphasize image

grain boundaries and decrease image noises allowing precise measurement of materials pores. The results indicated that the average pore diameter was 0.56 µm. The porosity is beneficial for sulfation-roasting-leaching once it increases the surface area, making the ore more reactive with the acid.

The XRD pattern of the laterite ore sample after deagglomeration with water and dry is shown in Fig. 3. The main phase present were chlorite ($\text{Mg}_6\text{Si}_4\text{O}_{10}(\text{OH})_8$), magnetite (Fe_3O_4), lizardita ($\text{Al}_3(\text{Si}_2\text{O}_5(\text{OH})_4$), goethite (FeOOH), hematite (Fe_2O_3) and quartz.

The chemical composition of the laterite ore sample was done after the deagglomeration of the particles in which 50% was below 135 µm. The magnesium, nickel,

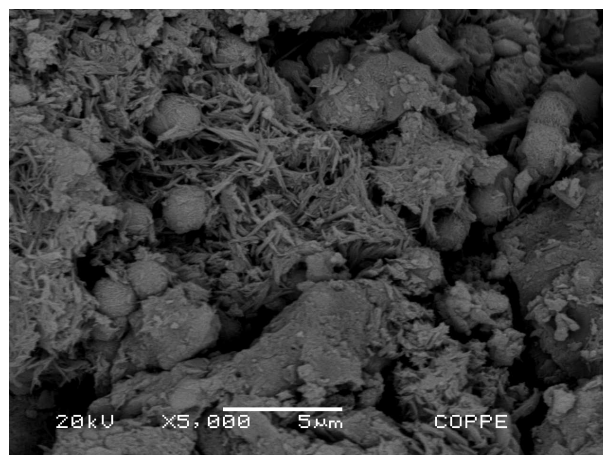


Fig. 1 SEM image of the laterite ore as received showing the particles agglomeration.

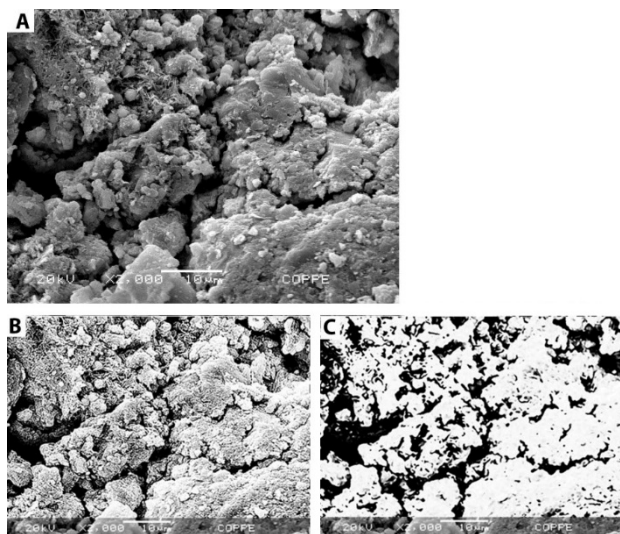


Fig. 2 SEM image of the laterite sample after deagglomeration with water previous (A) and after image processing (B – Threshold) and (C – image corrections).

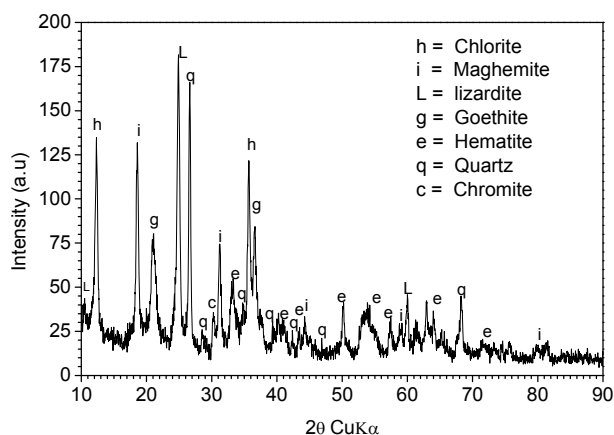


Fig. 3 XRD pattern of the laterite ore sample after deagglomeration with water and dry.

iron and cobalt content in laterite ore sample can be observed in Table 3. Note that the nickel content increased for the particle size smaller than 75 μm . This is due to the main nickel-bearing minerals in this ore are concentrated in smaller particle size fraction.

The XRD pattern of the laterite ore sample after sulfation, pre-roasting and roasting with 200% (w/w) can be seen in Fig. 4. New phases were identified and among them, some sulfates peaks like nickel, iron and magnesium sulfates.

The reactions of Eqs. (2) to (6) illustrate the main reactions occurring with the laterite ore during the steps of sulfation, pre-roasting, and roasting. Initially, the

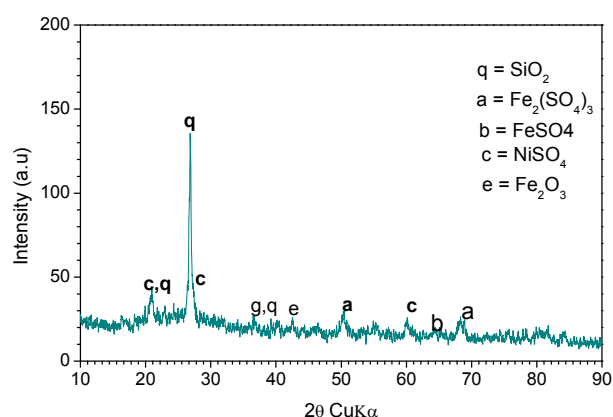
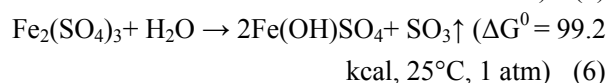
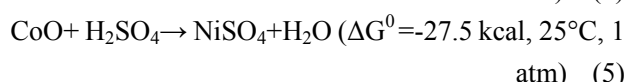
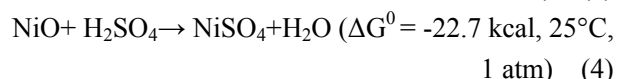
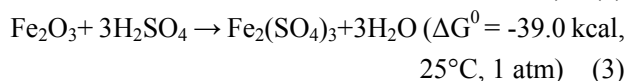
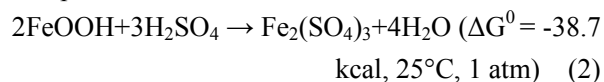
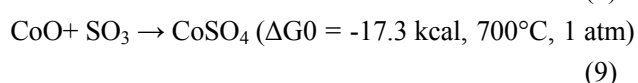
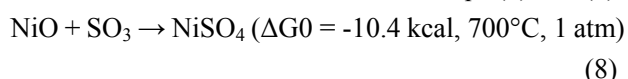


Fig. 3 XRD pattern of the laterite ore sample after sulfation, pre-roasting and roasting with 200% (w/w). Conditions: pre-roasting 100°C for 1 h and roasting at 620°C for 1 h.

preferred reactions are those shown in Eqs. (2) and (3) due to the high iron content in the ore. During the next step, the iron sulfates decompose liberating SO_3 which can react with other metals present in the ore as nickel and magnesium forming their sulfates. Despite the free energy is higher than zero at 25°C, it decreases as roasting temperature increases because the decomposition of iron sulfate is endothermic at 25°C.



In the roasting step the iron sulfates continuous to be decomposed according to Eq. (7), liberating SO_3 which can react with other metals present in the ore, increasing the degree of production of sulfates such as nickel and cobalt sulfates as shown in Eqs. (8) and (9).



The influence of the initial leaching pH in nickel and cobalt recoveries during the leaching step of the sulfation-roasting-leaching process of the laterite ore sample can be noted in Fig. 5. The analyses of this result allow concluding that leaching in initial pH too small, around 0.8, was not interesting due to the high iron content recovered. At pH in the range of 1.5-3, nickel recovery decreased. More than 62% of nickel was extracted with iron recovery below 3% at initial leaching pH equal 7 indicating to be this pH condition the most suitable for the sequence of leaching tests. The iron concentration in the pregnant leach solution tends to increase when the initial pH of the leaching solution decreases because of the increase in the solubility of iron species such as Fe^{+3} . Nickel, however, presents elevated solubility in the whole pH range investigated. Therefore, its recovery does not depend on the initial pH of leaching.

The nickel and iron recoveries for different sulfuric acid concentrations are presented in Fig. 6. It can be observed that nickel recovery was increased with the increase of sulfuric acid amount. According to literature [9-11], the increase of sulfuric acid above 50% present only a marginal effect on nickel recovery. In the present paper, however, the increase of nickel recovery for increasing amounts of sulfuric acid was almost linear. This behavior can be attributed to the

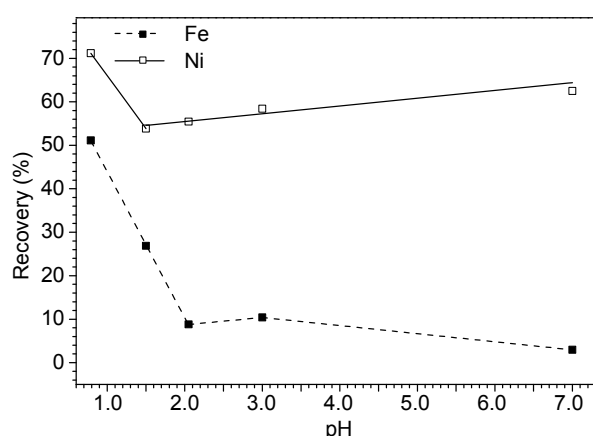


Fig. 4 Conditions: H_2O : 10% (w/w), H_2SO_4 : 34% (w/w), pre-roasting at 445°C for 20 minutes, roasting at 690°C for 20 minutes and leaching at 25°C for 30 minutes with a solid to liquid ratio of 1/40.

higher magnesium content in the ore sample, which was considerably higher than those found by other authors [2, 9, 11, 12]. Once the reaction of MgSO_4 formation during sulfation is thermodynamically more favorable than other sulfates formation and since it is a very stable compound which does not decompose in the temperature range used [13], a higher acid amount is demanded to achieve a satisfactory nickel recovery.

The effect of laterite ore sample comminution, to $-38\ \mu\text{m}$, on the nickel and iron recoveries is presented in Table 4. It can be observed, from Fig. 6 and Table 4, that nickel recovery was increased from 73.4% to 86.0% when the particle size was comminuted to 100% passing $38\ \mu\text{m}$. Furthermore, iron recovery decreased from 9.7% to 7.5%, representing a 22.7% drop. This behavior is due to the solid surface area increase caused by the ore sample comminution, turning the reactions of ferric sulfate decomposition along with the nickel sulfation faster.

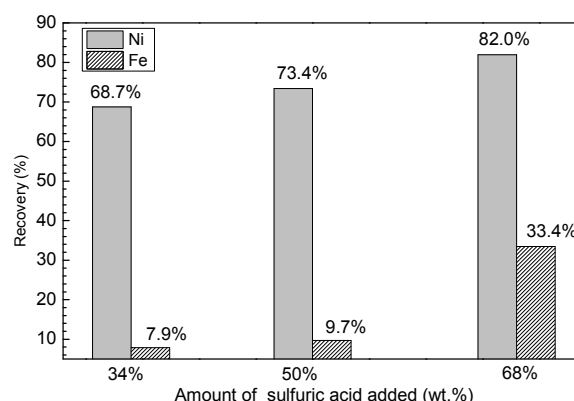


Fig. 6 Nickel and iron recoveries for different sulfuric acid concentrations. Conditions: H_2O : 40% (w/w), pre-roasting at 265°C for 20 minutes, roasting at 690°C for 20 minutes and leaching at 80°C for 30 minutes with a solid to liquid ratio of 1/40.

Table 4 Effect of laterite ore sample comminution, to $-38\ \mu\text{m}$, on the nickel and iron recoveries. Conditions: H_2O : 40% (w/w), H_2SO_4 : 50% (w/w), pre-roasting at 265°C for 20 minutes, roasting at 690°C for 20 minutes and leaching at 80°C for 30 minutes with a solid to liquid ratio of 1/40.

Element	Recovery (%)
Ni	86.0
Fe	7.5

The addition of Na_2SO_4 did not increase nickel recovery from the ore sample without a separation by particles size. This behavior can be attributed to the large particles size of the sample ($d_{50} = 135 \mu\text{m}$). However, it can be observed in Table 5 that for particles smaller than $75 \mu\text{m}$ nickel recovery was around 75% with an iron content in the pregnant leach solution of 3.95%, when Na_2SO_4 was added to the pugged sample previously to roasting. Without Na_2SO_4 additions, nickel recovery dropped almost 13%.

Table 5 Nickel and iron contents and recoveries of the laterite ore sample after the sulfation-roasting-leaching appliance for the fraction with particle size equal or smaller than $75 \mu\text{m}$. Conditions: H_2SO_4 : 50% (w/w), H_2O : 40% (w/w), pre-roasting at 265°C for 20 minutes, roasting at 690°C for 20 minutes and leaching at 80°C for 30 minutes with a solid to liquid ratio of 1/40.

Element	Content in PLS*(% (w/w))	Recovery (%)	Na_2SO_4 (w/w)
Fe	3.95	10.53	50.00
Ni	1.57	75.17	50.00
Fe	2.18	5.81	0.00
Ni	1.31	62.49	0.00

*Pregnant leaching solution

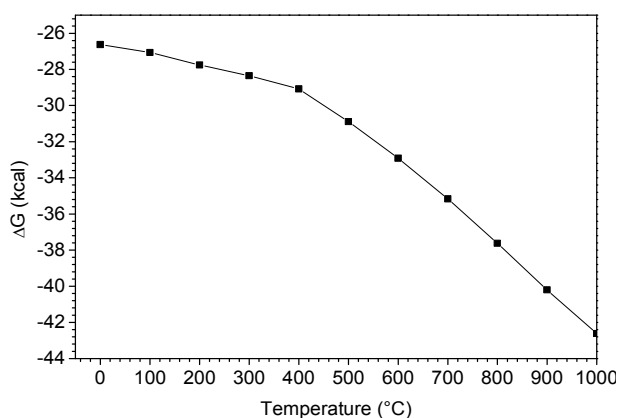


Fig. 7 Gibbs free energy in function of the temperature for the reaction: $\text{Na}_2\text{SO}_4 + \text{SO}_3 \rightarrow \text{Na}_2\text{S}_2\text{O}_7$.

4. Conclusion

It was found by image analysis that the nickel laterite ore sample has a high reactivity with sulfuric acid due to the large surface area existent caused by the high number of pores with small size.

Nickel recovery increased from 68.7% to 82% as the acid content increased from 34% (w/w) to 68% (w/w). The higher magnesium amount found in the sample (5.08%) influenced in the acid consumption once it can react preferably with the acid reducing the amount of

Some authors [9] reported that the additions of salts, as sodium sulfate can contribute to the increase of nickel recovery due to the formation of pyrosulfates during the roasting step. The pyrosulfates are stable in the temperature range of 0 to 800°C , as shown in Fig. 7. In this figure it can be also observed that the free energy change for reaction (10) is negative throughout all the temperature range considered (0 to 1000°C), becoming more negative as the temperature is increased.



free acid and turning necessary a higher amount of acid to extract nickel. After comminution of the ore sample to 100% passing in $38 \mu\text{m}$ before applying the sulfation-roasting-leaching process, the nickel recovery increased almost 13% and the iron recovery decreased more than 22%.

The Na_2SO_4 addition previously the roasting steps for the ore fraction with the particle size equal or smaller than $75 \mu\text{m}$ allowed the nickel recovery to increase from 62.5% to 75.2% and a decrease in iron recovery from 9.7% to 7.5% using 50% (w/w) of sulfuric acid.

References

- [1] D. Q. Zhu, Y. Cui, S. Hapugoda, K. Vining and J. Pan, Mineralogy and crystal chemistry of a low grade nickel laterite ore, *Trans Nonferrous Met Soc China* (English Ed (2012) (22) 907-916, doi: 10.1016/S1003-6326(11)61264-8.
- [2] D. Georgiou and V. G. Papangelakis, Sulphuric acid pressure leaching of a limonitic laterite: chemistry and kinetics, *Hydrometallurgy* (1998) (49) 23-46, doi: 10.1016/S0304-386X(98)00023-1.

- [3] G. Senanayake, J. Childs, B. D. Akerstrom and D. Pugaev, Reductive acid leaching of laterite and metal oxides — A review with new data for Fe(Ni,Co)OOH and a limonitic ore, *Hydrometallurgy* (2011) (110) 13-32, doi: 10.1016/j.hydromet.2011.07.011.
- [4] A. Oxley and N. Barcza, Hydro-pyro integration in the processing of nickel laterites, *Miner Eng* (2013) (54) 2-13, doi: 10.1016/j.mineng.2013.02.012.
- [5] F. K. Crundwell, M. S. Moats, V. Ramachandran, T. G. Robinson and W. G. Davenport, *Extractive Metallurgy of Nickel, Cobalt and Platinum Group Metals*, 2011, pp. 1-18.
- [6] T. Norgate and S. Jahanshahi, Assessing the energy and greenhouse gas footprints of nickel laterite processing, *Miner Eng* (2011) (24) 698-707, doi: 10.1016/j.mineng.2010.10.002.
- [7] D. H. Rubisov, J. M. Krowinkel and V. G. Papangelakis, Sulphuric acid pressure leaching of laterites — universal kinetics of nickel dissolution for limonites and limonitic/saprolitic blends, *Hydrometallurgy* (2000) (58) 1-11, doi: 10.1016/S0304-386X(00)00094-3.
- [8] K. Liu, Q. Chen and H. Hu, Comparative leaching of minerals by sulphuric acid in a Chinese ferruginous nickel laterite ore, *Hydrometallurgy* (2009) (98) 281-286, doi: 10.1016/j.hydromet.2009.05.015.
- [9] Y. V. Swamy, B. B. Kar and J. K. Mohanty, Overburden by sulphatization roasting, *Pyrometallurgy Div* (2003) (13) 1635-1640.
- [10] E. Büyükakinci and Y. A. Topkaya, Extraction of nickel from lateritic ores at atmospheric pressure with agitation leaching, *Hydrometallurgy* (2009) (97) 33-38, doi: 10.1016/j.hydromet.2008.12.014.
- [11] Y. V. Swamy, B. B. Kar and J. K. Mohanty, Some aspects of nickel extraction from chromitiferous overburden by sulphatization roasting, *Miner Eng*, 2000.
- [12] G. Li, M. Rao, T. Jiang, Q. Huang and Z. Peng, Leaching of limonitic laterite ore by acidic thiosulfate solution, *Miner Eng* (2011) (24) 859-863, doi: 10.1016/j.mineng.2011.03.010.
- [13] H. Emons, G. Ziengenbalg, R. Naumann and F. Paulik, Thermal decomposition of the magnesium sulphate hydrates under quasi-isothermal and quasi-isobaric conditions, *J Therm Anal* (1990) (36).